DOI: 10.1002/cmdc.200700348

Discovery of VHR Phosphatase Inhibitors with Micromolar Activity based on Structure-Based Virtual Screening

Hwangseo Park,*[a] Suk-Kyeong Jung,[b] Dae Gwin Jeong,[c] Seong Eon Ryu,[c] and Seung Jun Kim*[b]

Protein tyrosine phosphatases (PTPs) are a family of closely related key regulatory enzymes and are responsible for the dephosphorylation of phosphotyrosine residues in their protein substrates. So far much evidence has been reported in support of the correlation between malfunctions in PTP activity and various diseases including cancer, neurological disorders, and diabetes.[1] This has made PTPs promising targets for therapeutic intervention. Among the variety of PTPs, vaccinia H1-related (VHR) phosphatase is a dual-specificity phosphatase (DSP) that dephosphorylates the activated ERK and JNK MAP kinases and thereby weakens the ERK signaling cascade in mammalian cells.[2,3]

Recently Rahmouni et al. reported that the human VHR phosphatase was involved in the regulation of cell-cycle progression and was itself modulated during the cell cycle.[4] Using RNA interference, they also showed that cells lacking VHR arrested at the G1-S and G2-M transitions of the cell cycle with a decreased telomerase activity. This line of experimental evidence indicates that VHR can serve as a therapeutic target for cancer. Furthermore, the VHR activity has been known to be promoted by ZAP-70, a spleen tyrosine kinase (Syk)-related tyrosine kinase, which plays a critical role in the immune response of activated T cells,[5] or by the interaction with vaccinia-related kinase 3 (VRK3).[6] The involvement of VHR in immune response also supports the possibility that it can be a potential target for drug discovery. Besides the pharmaceutical interest, specific inhibitors of VHR are expected to be useful for revealing the physiological functions of VHR and ERK signaling.

The X-ray crystal structure of VHR exhibited a conserved structural scaffold for both DSPs and PTPs.[7] A shallow active site pocket in VHR is consistent with its broad substrate specificity for the hydrolysis of phosphorylated serine, threonine, and tyrosine residues. Positively charged crevices near the active site were invoked to explain the preference of VHR for the substrates with two phosphorylated residues. In the crystal structure, the catalytic residue Cys124 resides in close proximity to the central sulfur atom of the substrate analogue at a distance of 3.65 Å. This supports the possibility that Cys124 acts as a nucleophile attacking the phosphorus atom of a substrate to form a phosphoenzyme intermediate.[8] The X-ray crystal structure also showed that the negatively charged oxygen atoms of the substrate analogue should be stabilized in the active site through the formation of multiple hydrogen bonds with backbone amide groups and the side chain of Arg130. These structural features may serve as key information for the discovery of small molecules modulating the catalytic activity of VHR.

Despite a series of experimental evidence for the involvement of VHR in several human diseases, only a few VHR inhibitors have been discovered so far. These include natural products[9,10] and synthetic compounds such as tetronic acid, RK-682, and benzofuran.[11–14] Recently, Shi et al. identified five new inhibitors of VHR based on structure-based virtual screening with docking simulations in combination with diffusion-edited NMR spectroscopy experiments.[15] Subsequent enzymatic assays showed that one of them could inhibit VHR at the micromolar level. The calculated binding mode of the inhibitor was consistent with that in the X-ray crystal structure of VHR in complex with a substrate analogue.

In the present study, we identify the novel classes of VHR inhibitors by means of a structure-based drug design protocol involving the virtual screening with docking simulations and in vitro enzyme assay. Virtual screening with docking simulation has not always been successful because of the use of the inaccurate scoring functions.[16] The characteristic feature that discriminates our virtual screening approach from the others lies in the implementation of an accurate solvation model in calculating the binding free energy between VHR and its putative ligands, which would have an effect of increasing the hit rate in the enzyme assay.[17,18] The reason for this lies in that the overestimation of the binding affinity of a ligand with many polar atoms can be avoided by including its desolvation energy in the scoring function. It will be shown that the docking simulation with the improved scoring function can be a useful tool for elucidating the activities of the identified inhibitors, as well as for enriching the chemical library with molecules that are likely to have biological activities.

Of the 85000 compounds subject to the virtual screening with docking simulations, 200 top-scored compounds were selected as virtual hits. 194 of them were available from the compound supplier and were tested for inhibitory activity against VHR by in vitro enzyme assay. The inhibition assay was performed in duplicates at all concentrations of the inhibitors and

[a] *Prof. H. Park*
Department of Bioscience and Biotechnology
Sejong University
98 Kunja-Dong, Kwangjin-Ku, Seoul 143-747 (Korea)
Fax: (+82) 2-3408-4334
E-mail: hspark@sejong.ac.kr

[b] *S.-K. Jung, Dr. S. J. Kim*
Translational Research Center
Korea Research Institute of Bioscience and Biotechnology
52 Eoeun-Dong, Yuseong-Gu, Daejeon 305-333 (Korea)
Fax: (+82) 42-860-4598
E-mail: ksj@kribb.re.kr

[c] *D. G. Jeong, Dr. S. E. Ryu*
Systemic Proteomics Research Center
Korea Research Institute of Bioscience and Biotechnology
52 Eoeun-Dong, Yuseong-Gu, Daejeon 305-333 (Korea)

Supporting information for this article is available on the WWW under http://www.chemmedchem.org or from the author.

the average values were used as data points. As a result, we identified 23 compounds that inhibited the catalytic activity of VHR by more than 50% at the concentration of 50 μM. Among them, six compounds revealed a high potency with more than 70% inhibition at the same concentration and were selected to determine IC_{50} values. The chemical structures and the inhibitory activities of the newly identified inhibitors are shown in Figure 1 and Table 1, respectively. The structures of the remaining 17 compounds revealing more than 50% inhibition of VHR activity at 50 μM are shown in Supporting Information. We note that compounds **1** and **2** share a common [2-(2,5-dioxo-imidazolidin-4-ylidenemethyl)-pyrrol-1-yl]-benzoic acid scaffold and exhibit the highest potency with single-digit IC_{50} values. The calculated binding free energies of these two potent inhibitors are also similar: 21.9 and 22.1 kcal mol^{-1} for **1** and **2**, respectively. Both **3** and **6** possess the 1-(3,4-dihydroxyphenyl)-2-(4*H*-[1,2,4]triazol-3-ylsulfanyl)-ethanone group as a common scaffold. More than threefold higher activity of **3** than **6** indicates that the size of the hydrophobic group substituted on the triazole ring should be limited. Compounds **4** and **5** reveal a similar inhibitory activity of 20–25 μM, either of which may be viewed as an independent inhibitor scaffold. The six inhibitors shown in Figure 1 can thus be divided into four structural classes. To the best of our knowledge, all of these compounds have not been reported as VHR inhibitors so far. Judging from the potency and the structural diversity, all of the newly identified inhibitor scaffolds seem to deserve further development by structure–activity relationship (SAR) or de novo design methods to optimize their inhibitory activities.

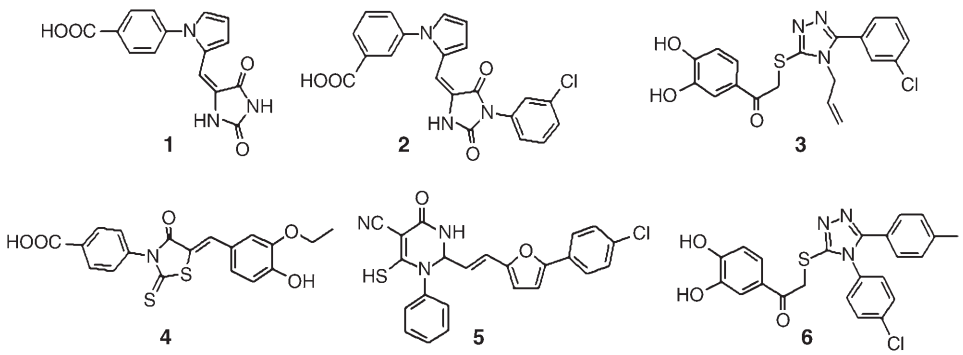

Figure 1. Chemical structures of the newly identified VHR inhibitors.

Table 1. The inhibitory activities of compounds **1**–**6** against VHR.[a]

compd.	% inhibition at 50 μM	IC_{50} [μM]
1	82.8	3.7
2	83.5	4.7
3	77.2	13.9
4	72.1	20.0
5	74.7	24.2
6	70.9	46.5

[a] At all concentrations of the inhibitors, the inhibition assay was performed in duplicates.

To obtain some energetic and structural insight into the inhibitory mechanisms by the identified inhibitors of VHR, their binding modes in the active site were investigated using the AutoDock program with the procedure described in the Experimental Section. The calculated binding mode of **1** in the active site of VHR is shown in Figure 2. We see that the carboxylate group of the inhibitor points toward the catalytic residue Cys124 at a distance of 3–4 Å. It is also noted that one of the carboxylate oxygens receives two hydrogen bonds from the backbone amide group and the side-chain NE atom of Arg130. The other carboxylate oxygen also forms two hydrogen bonds with the side-chain guanidium group of Arg130 and backbone amide group of Arg125. As the carboxylate group of **1** resides in close proximity to Cys124 and is stabilized by the formation of multiple hydrogen bonds at the active site, the benzoate moiety seems to be an effective surrogate for the substrate phosphate group binding tightly in the active site of VHR and thereby inhibiting its catalytic activity. The inhibitor **1** can be further stabilized by the hydrophobic interactions of the imidazolidine-2,4-dione moiety with the side chains of Leu25, Pro26, and Tyr128. Judging from the overall structural features of the VHR–**1** complex derived from docking simulations, the micromolar inhibitory activity of **1** is likely to stem from the multiple hydrogen bonds and hydrophobic interactions established simultaneously in the active site.

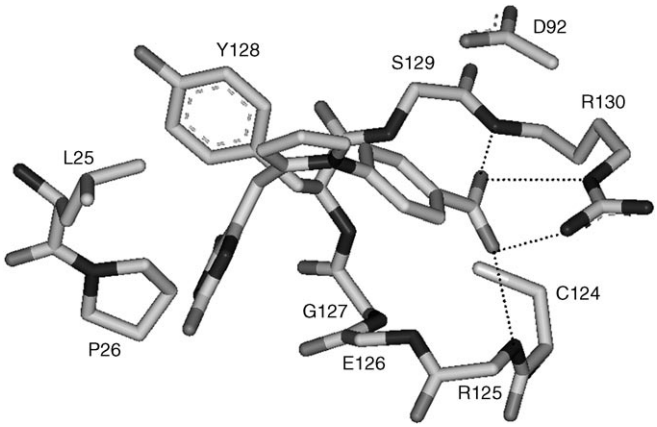

Figure 2. Binding mode of **1** in the active site of VHR. Each dotted line indicates a hydrogen bond.

Figure 3 shows the lowest-energy conformation of **2** in the active site of VHR obtained from docking simulations. The binding mode of **2** is similar to that of **1** in that the benzoate

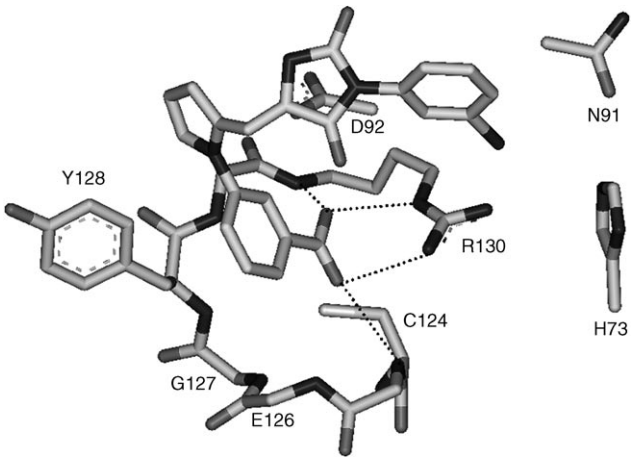

Figure 3. Binding mode of **2** in the active site of VHR. Each dotted line indicates a hydrogen bond.

group points toward the catalytic residue Cys 124 with the terminal carboxylate group being stabilized by four hydrogen bonds with the backbone amide groups of Arg 125 and the side-chain guanidium group of Arg 130. However, the binding mode of **2** differs from that of **1** in that the imidazolidine-2,4-dione group is exposed to bulk solvent instead of being accommodated in a small binding pocket adjacent to the catalytic site. This is likely to have an effect of lowering the inhibitory activity of **2** and apparently is due to the substitution of a large chlorophenyl group at the terminal amidic nitrogen. As a consequence of the substitution, however, the terminal chlorophenyl moiety is stabilized in another binding pocket including the side chains of His 73 and Asn 91. The establishment of this new hydrophobic interaction seems to compensate for the loss of the interaction between imidazolidine-2,4-dione group and active-site residues, which can be an explanation for the similarity in inhibitory activities of **1** and **2**.

In summary, we have identified six new inhibitors of VHR by applying the structure-based virtual screening with docking simulations under consideration of the effects of ligand solvation in the scoring function. These inhibitors exhibit a significant potency with IC_{50} values ranging from a 1 to 50 μM and can be categorized into four structural classes. Considering the novelty and the potency, each of the newly discovered inhibitor scaffolds deserves further development by structure–activity relationship studies or de novo design methods. Detailed binding mode analyses with docking simulation show that the inhibitors can be stabilized by the simultaneous establishment of multiple hydrogen bonds and van der Waals contacts in the active site.

Experimental Section

Virtual screening of VHR inhibitors

The 3-D coordinates in the X-ray crystal structure of VHR in complex with a substrate analogue (PDB code: 1VHR)[7] were selected as the receptor model in the virtual screening with docking simulations. After removing the ligand and solvent molecules, hydrogen atoms were added to each protein atom. Special attention was paid to assign the protonation states of the ionizable Asp, Glu, His, and Lys residues. The side chains of Asp and Glu residues were assumed to be neutral if one of their carboxylate oxygens pointed toward a hydrogen-bond accepting group including the backbone aminocarbonyl oxygen at a distance within 3.5 Å, a generally accepted distance limit for a hydrogen bond of moderate strength.[19] Similarly, the lysine side chains were assumed to be protonated unless the NZ atom was in proximity of a hydrogen-bond donating group. The same procedure was also applied to determine the protonation states of ND and NE atoms in His residues.

The docking library for VHR comprising about 85 000 compounds was constructed from the latest version of the chemical database distributed by Interbioscreen (http://www.ibscreen.com) containing approximately 30 000 natural and 320 000 synthetic compounds. The selection was based on the drug-like filters that adopt only the compounds with physicochemical properties of potential drug candidates[20] and without reactive functional group(s). All of the compounds included in the docking library were then subjected to the Corina program to generate their 3-D atomic coordinates, followed by the assignment of Gasteiger–Marsilli atomic charges.[21] We used the AutoDock program[22] in the virtual screening of VHR inhibitors because the outperformance of its scoring function over those of the others had been shown in several target proteins.[23] AMBER force field parameters were assigned for calculating the van der Waals interactions and the internal energy of a ligand as implemented in the AutoDock program.

In the actual docking simulation of the compounds in the docking library, we used the empirical scoring function improved by the implementation of a new solvation model for a compound. The desolvation term in the original AutoDock was thus set equal to zero. The modified scoring function has the following form:

$$\Delta G_{bind}^{aq} = W_{vdW}\sum_{i=1}\sum_{j>i}\left(\frac{A_{ij}}{r_{ij}^{12}}-\frac{B_{ij}}{r_{ij}^{6}}\right) + W_{hbond}\sum_{i=1}\sum_{j>i}E(t)\left(\frac{C_{ij}}{r_{ij}^{12}}-\frac{D_{ij}}{r_{ij}^{10}}\right) + W_{elec}\sum_{i=1}\sum_{j>i}\frac{q_i q_j}{\varepsilon(r_{ij})r_{ij}} + W_{tor}N_{tor} + W_{sol}\sum_{i=1}S_i\left(Occ_i^{\max}-\sum_{j>i}V_j e^{-\frac{r_{ij}^2}{2\sigma^2}}\right) \quad (1)$$

where W_{vdW}, W_{hbond}, W_{elec}, W_{tor}, and W_{sol} are the weighting factors of van der Waals, hydrogen bond, electrostatic interactions, torsional term, and desolvation energy of an inhibitor, respectively. r_{ij} represents the interatomic distance, and A_{ij}, B_{ij}, C_{ij}, and D_{ij} are related to the depths of the potential energy well and the equilibrium separations between the two atoms. The hydrogen bond term has an additional weighting factor, $E(t)$, representing the angle-dependent directionality. With respect to the distance-dependent dielectric constant, $\varepsilon(r_{ij})$, a sigmoidal function proposed by Mehler et al.[24] was used in computing the interatomic electrostatic interactions between VHR and a putative ligand. In the entropic term, N_{tor} is the number of sp^3 bonds in the ligand. In the desolvation term, S_i and V_i are the solvation parameter and the fragmental volume of atom i,[25] respectively, whereas Occ_i^{max} stands for the maximum atomic occupancy. In the calculation of molecular solvation free energy term in Equation (1), we used the atomic parameters recently developed by Kang et al.[26] because those of the atoms other than carbon were unavailable in AutoDock. This modification of the solvation free energy term is expected to increase the accuracy in virtual screening because the underestimation of ligand solvation often leads to the overestimation of the binding affinity of a ligand with many polar atoms.[17,18]

The docking simulation of a compound in the docking library started with the 3-D grid calculations of the interaction energy for all of the possible atom types present in the chemical database. These uniquely defined potential grids for the receptor protein were then used in common for docking simulations of all compounds in the docking library. As the center of the common grids in the active site, we used the center of mass coordinates of the docked structure of the probe molecule, GATPT, whose inhibitory activity and binding mode in the active site of VHR had been investigated by docking simulations.[15] The calculated grid maps were of dimension $61\times61\times61$ points with the spacing of 0.375 Å, yielding a receptor model that includes atoms within 22.9 Å of the grid center. This radius to define the grid maps is sufficient to include the entire part of VHR phosphatase because the diameter of the protein amounts to at most 48 Å. For each compound in the docking library, ten docking runs were performed with the initial population of 50 individuals. Maximum number of generations and energy evaluation were set to 27000 and 2.5×10^5, respectively. Docking simulations with AutoDock were then carried out in the active site of VHR to score and rank the compounds in the docking library according to their calculated binding affinities.

In vitro enzyme assay

VHR protein was subcloned into pET28a and overexpressed using *Escherichia coli* BL21(DE3) strain. Cells were grown at 291 K after induction with 0.1 mM IPTG for 12 h. His-tagged VHR was purified by nickel-affinity chromatography and dialyzed against buffer containing 20 mM Tris-HCl (pH 8.0), 0.2 M NaCl, and 5 mM DTT. 194 compounds selected from virtual screening were evaluated for their in vitro inhibitory activity against the recombinant human VHR. Assays were performed by monitoring the hydrolysis of 6,8-difluoro-4-methyl-umbelliferyl phosphate (DiFMUP) using a spectrofluorometric assay. Briefly, purified VHR (5 nM), DiFMUP (10 μM), and desired inhibitor were incubated in the reaction mixture containing 20 mM Tris-HCl (pH 8.0), 0.01% Trition X-100, and 5 mM DTT for 20 min. The reaction was stopped by the addition of sodium orthovanadate (1 mM). The phosphatase activities were checked by the absorbance changes caused by hydrolysis of the substrate at 460 nm and IC_{50} values were determined from direct regression curve analysis.

Acknowledgements

This work was supported by the grant from KRIBB Research Initiative Program.

Keywords: docking · inhibitors · solvation · VHR phosphatase · virtual screening

[1] L. Bialy, H. Waldmann, *Angew. Chem.* **2005**, *117*, 3880–3906; *Angew. Chem. Int. Ed.* **2005**, *44*, 3814–3839.
[2] A. Alonso, M. Saxena, S. Williams, T. Mustelin, *J. Biol. Chem.* **2001**, *276*, 4766–4771.
[3] J. L. Todd, K. G. Tanner, J. M. Denu, *J. Biol. Chem.* **1999**, *274*, 13271–13280.
[4] S. Rahmouni, F. Cerignoli, A. Alonso, T. Tsutji, R. Henkens, C. Zhu, C. Louis-dit-Sully, M. Moutschen, W. Jiang, T. Mustelin, *Nat. Cell Biol.* **2006**, *8*, 524–531.
[5] A. Alonso, S. Rahmouni, S. Williams, M. van Stipdonk, L. Jaroszewski, A. Godzik, R. T. Abraham, S. P. Schoenberger, T. Mustelin, *Nat. Immunol.* **2003**, *4*, 44–48.
[6] T. H. Kang, K. T. Kim, *Nat. Cell Biol.* **2006**, *8*, 863–869.
[7] J. Yuvaniyama, J. M. Denu, J. E. Dixon, M. A. Saper, *Science* **1996**, *272*, 1328–1331.
[8] G. Zhou, J. M. Denu, L. Wu, J. E. Dixon, *J. Biol. Chem.* **1994**, *269*, 28084–28090.
[9] E. Y. Bae, H. Oh, W. K. Oh, M. S. Kim, B. S. Kim, B. Y. Kim, C. B. Sohn, H. Osada, J. S. Ahn, *Planta Med.* **2004**, *70*, 869–870.
[10] M. S. Lee, W. K. Oh, B. Y. Kim, S. C. Ahn, D. O. Kang, C. B. Sohn, H. Osada, J. S. Ahn, *Planta Med.* **2002**, *68*, 1063–1065.
[11] K. Ueda, T. Usui, H. Nakayama, M. Ueki, K. Takio, M. Ubukata, H. Osada, *FEBS Lett.* **2002**, *525*, 48–52.
[12] T. Usui, S. Kojima, S. Kidokoro, K. Ueda, H. Osada, M. Sodeoka, *Chem. Biol.* **2001**, *8*, 1209–1220.
[13] M. Sodeoka, R. Sampe, S. Kojima, Y. Baba, T. Usui, K. Ueda, H. Osada, *J. Med. Chem.* **2001**, *44*, 3216–3222.
[14] J. S. Lazo, R. Nunes, J. J. Skoko, P. E. Queiroz de Oliveira, A. Vogt, P. Wipf, *Bioorg. Med. Chem.* **2006**, *14*, 5643–5650.
[15] Z. Shi, S. Tabassum, W. Jiang, J. Zhang, S. Mathur, J. Wu, Y. Shi, *ChemBioChem* **2007**, *8*, 2092–2099.
[16] G. L. Warren, C. W. Andrews, A.-M. Capelli, B. Clarke, J. LaLonde, M. H. Lambert, M. Lindvall, N. Nevins, S. F. Semus, S. Senger, G. Tedesco, I. D. Wall, J. M. Woolven, C. E. Peishoff, M. S. Head, *J. Med. Chem.* **2006**, *49*, 5912–5931.
[17] X. Zou, Y. Sun, I. D. Kuntz, *J. Am. Chem. Soc.* **1999**, *121*, 8033–8043.
[18] B. K. Shoichet, A. R. Leach, I. D. Kuntz, *Proteins Struct. Funct. Genet.* **1999**, *34*, 4–16.
[19] G. A. Jeffrey, *An introduction to hydrogen bonding*, Oxford University Press, Oxford, **1997**, pp. 79–97.
[20] C. A. Lipinski, F. Lombardo, B. W. Dominy, P. J. Feeney, *Adv. Drug Delivery Rev.* **1997**, *23*, 3–25.
[21] J. Gasteiger, M. Marsili, *Tetrahedron* **1980**, *36*, 3219–3228.
[22] G. M. Morris, D. S. Goodsell, R. S. Halliday, R. Huey, W. E. Hart, R. K. Belew, A. J. Olson, *J. Comput. Chem.* **1998**, *19*, 1639–1662.
[23] H. Park, J. Lee, S. Lee, *Proteins Struct. Funct. Genet.* **2006**, *65*, 549–554.
[24] E. L. Mehler, T. Solmajer, *Protein Eng.* **1991**, *4*, 903–910.
[25] P. F. W. Stouten, C. Frömmel, H. Nakamura, C. Sander, *Mol. Simul.* **1993**, *10*, 97–120.
[26] H. Kang, H. Choi, H. Park, *J. Chem. Inf. Model.* **2007**, *47*, 509–514.

Received: December 6, 2007
Revised: January 9, 2008
Published online on January 31, 2008

